transiently expressed in the now-closed neural tube. An important facet of the expression pattern of *FGF-19* is that, as the authors demonstrate, it colocalizes with otic-inducing activity. If the *FGF-19*–expressing mesoderm is cocultured with early embryonic ectoderm in the laboratory, then the expression of a broad range of otic markers is induced in this tissue, including the formation of auditory hair cells, which mark the terminal stages of inner ear differentiation. By contrast, other mesoderm that did not express *FGF-19* could not induce otic markers in this ectoderm. Similarly, otic markers could be induced in early ectoderm when it was cocultured with *FGF-19*–expressing neuroectoderm and its adjacent mesoderm. Although *FGF-19* expression colocalizes with otic inducing activity, Ladher *et al.* found that the FGF-19 protein alone could not promote the expression of otic markers in either nonotic ectoderm or presumptive otic ectoderm. This protein could, however, elicit an otic response in these tissues if neural tissue was included. Thus, FGF-19 itself can only direct otic development provided another neural-derived signal is also present.

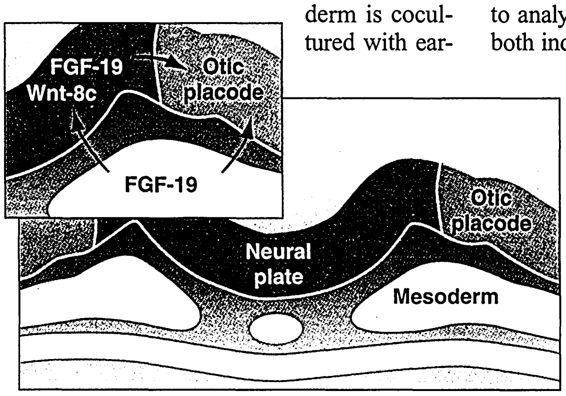

Breaking the silence. A transverse section through a chick embryo showing the relative positions of the mesoderm, neural plate, and presumptive otic placode, which develops into the inner ear. Also shown are the signaling molecules that induce formation of the otic placode. First, the mesoderm produces FGF-19, which then signals to the overlying neural plate and ectoderm. The neural tissue then produces Wnt-8c, which acts in concert with FGF-19 to induce the adjacent ectoderm to become the otic placode.

Taking their cue from studies in the frog *Xenopus* showing that FGFs often work together with another group of signaling molecules (the Wnts), Ladher and colleagues investigated whether Wnt-8c was the second otic inducer. This signaling molecule was already known to be expressed in the area of the neural tube closest to the region (*3*) where the otic placode forms. On closer scrutiny, they found that *Wnt-8c* was expressed in the neural tissue overlying the *FGF-19*–expressing mesoderm, and that at later stages Wnt-8c and FGF-19 were located in the same area of neural tissue. These authors also showed that FGF-19 could induce the expression of *Wnt-8c* in early embryonic ectoderm in culture. Thus, Wnt-8c is a prime candidate for the neural signal working with FGF-19 to induce the otic placode. So, they proceeded to analyze the abilities of these two factors, both independently and together, to promote otic development. As before, they found that FGF-19 alone could not promote otic development, but that Wnt-8c, on its own, induced the expression of one otic marker, *FGF-3*. However, Wnt-8c was unable to direct the robust expression of any other otic marker. In contrast, if ectoderm was treated with both FGF-19 and Wnt-8c, there was strong expression of a gamut of otic markers and the ectoderm began to acquire the morphology of the otic placode. It is noteworthy that the otic induction driven by the combined action of FGF-19 and Wnt-8c is direct, and does not require the prior induction of neural tissue. However, because these two factors did not elicit the formation of cochlear inner hair cells in the cultured ectodermal explants, other signals may be required to promote full inner ear development.

Although previous investigations of otic induction identified the mesoderm and the neural tissue as inducers, the new work provides us with a clearer picture of how the inducer tissues initiate inner ear development (see the figure). This process begins with the mesoderm: Through production of FGF-19, the mesoderm signals to the overlying neural plate inducing the expression of *Wnt-8c* in this tissue, and to the ectoderm, which then gives rise to the otic placode. Subsequently, Wnt-8c and FGF-19, emanating from the hindbrain, act together on this ectoderm to induce the otic placode and thus to initiate inner ear development.

The fact that FGF-19 can induce expression of *Wnt-8c* in presumptive neuroectoderm also suggests that FGF-19 plays a part in patterning the neural tube. This is in keeping with previous work on neural patterning that implicated an undefined FGF activity in regionalizing the neural plate into midbrain and hindbrain territories (*4*). Hence, it is likely that FGF-19 is acting specifically to pattern the central hindbrain territory alongside which the otic placode forms. It is within this territory that the auditory nuclei of the brainstem arise (*5*). Thus, FGF-19 could be pivotal in ensuring the coordinated development of both the inner ear and its neuronal transducing apparatus.

References

1. A. G. Jacobson, *Science* **152**, 25 (1966).
2. R. K. Ladher, K. U. Anakwe, A. L. Gurney, G. C. Schoenwolf, P. H. Francis-West, *Science* **290**, 1965 (2000).
3. C. R. Hume, J. Dodd, *Development* **119**, 1147 (1993).
4. J. Muhr *et al.*, *Neuron* **23**, 689 (1999).
5. F. Marin, L. Puelles, *Eur. J. Neurosci.* **7**, 1714 (1995).

PERSPECTIVES: PALEOCLIMATE

Glacial Climate Instability

Laurent Labeyrie

Throughout the last glacial period, rapid climatic changes left their mark in the glacial ice in Greenland. During each of these Dansgaard-Oeschger (D-O) events, named in honor of the initial leaders in their study, an initial warming of 10°C or more within a few decades was followed by a gradual cooling over about 1000 years. Twenty-one such events occurred between 75,000 and 15,000 years ago (75 to 15 ka). Because the events were so similar over tens of thousands of years, they are ideal targets for testing our understanding of climate change and developing climatic change models. Important steps toward understanding D-O events, particularly regarding the role of the low latitudes, are now reported by Hughen *et al.* (*1*) on page 1951 and Peterson *et al.* (*2*) on page 1947 of this issue.

Preliminary low-resolution studies (with a resolution of ~500 years) of North Atlantic sediment cores have indicated that D-O events are probably driven by oscillations of the polar front and associated changes in the convective thermohaline ocean circulation. The slow cooling may be caused by input of melt water from continental ice sheets into the surface waters of the high-latitude Atlantic Ocean, interrupting deep water formation. At the end of the melt water event, the thermohaline circulation would restart rapidly, at the same time as a northward shift of the polar front and warm conditions over Greenland (*3–6*). Low latitudes may also be affected but are not necessarily in phase with the high latitudes (*7*).

To fully understand the mechanism that drives D-O events requires well-dated ocean paleoclimatic records with much higher resolution (a few decades to a century). Such

---

The author is at the Université Paris-Sud and the Laboratoire des Sciences du Climat et de l'Environnement, CNRS-CEA, 91198 Gif-sur-Yvette, France. E-mail: laurent.labeyrie@lsce.cnrs-gif.fr

high-resolution sediment records require high sedimentation rates (20 cm or more per 1000 years) and minimum perturbation by benthic (bottom-dwelling) organisms. The ODP (Ocean Drilling Program) and IMAGES (International Marine Global Change Study) (*8*) play major roles in the acquisition of the necessary sediment cores, but few ideal coring locations have been identified, among them the Cariaco Basin in the Southern Caribbean Sea and the Santa Barbara basin along the California coast. Both allow the study of low-latitude climate during D-O events. This is important because the low latitudes may play a key role in driving D-O events. Any satisfactory D-O mechanism must explain the interaction between low and high latitudes.

As indicated above, oscillations created by the high-latitude interactions between ice sheets, surface water, albedo, atmospheric dynamics, and deep water convection and transport could explain rapid and large-amplitude shifts in the polar front and air temperature. Lower latitudes could be affected indirectly through a southward shift of the Intertropical Convergence Zone (ITCZ) and the associated trade wind belt at times of maximum extension of the polar vortex. If this mechanism is correct, then climatic changes at low latitudes of the Northern Hemisphere should lag behind those in high-latitude temperature.

But it is also possible that the low latitudes play a major role in at least one aspect of the oscillation cycle. Water vapor (snow) transfer through the atmosphere to the northern ice sheets could increase dramatically during glacial periods. As long as this water remains on the continents as ice, the thermohaline circulation stays active. But when the ice sheet grows until it becomes unstable, massive ice-rafting (Heinrich) events will cause a decrease in thermohaline circulation because the fresher, less salty waters do not sink to the bottom. This would allow more heat to accumulate at low latitudes, resulting in more evaporation and thus new growth of ice. In this scenario, maximum warmth at low latitude would be in phase with increasing ice sheet size and decreasing high-latitude temperature. This pattern corresponds to observations for the Younger Dryas period at the end of the last glacial, 13 to 11 ka (*7*).

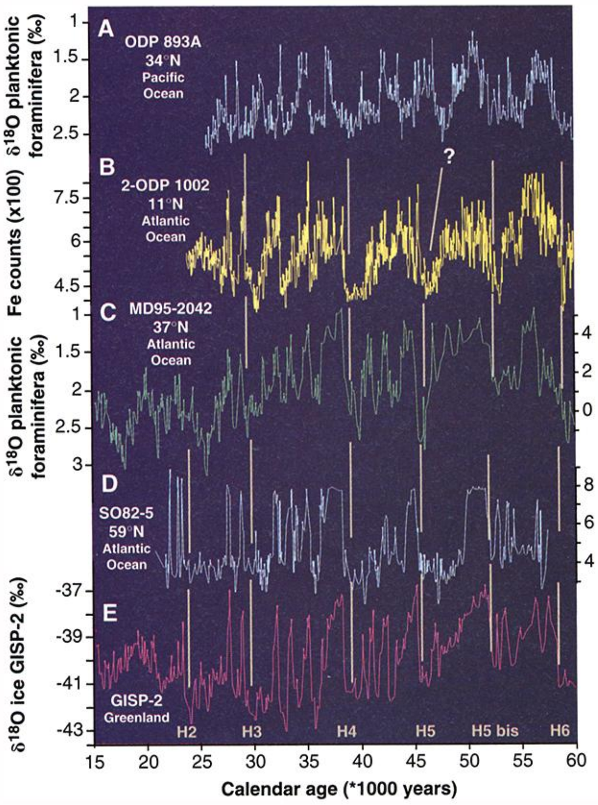

Comparison of climatic change records for the last glacial period. Foraminiferal $\delta^{18}O$ is a proxy for relative sea surface temperature (SST) changes. Fe content is a proxy for rain and detrital fluxes from the nearby continent. Time scales derived from AMS ^{14}C dating and correlation with the GISP-2 $\delta^{18}O$ record (*10, 11*). **(A)** $\delta^{18}O$ of planktonic foraminifera from ODP hole 893A, Santa Barbara basin (*12*). **(B)** Fe record from ODP hole 1002C, Cariaco Basin (*2*). **(C)** $\delta^{18}O$ of planktonic foraminifera from core MD95-2042, Iberian margin (*13*). **(D)** SST record derived from foraminifera species distribution in core SO82-5, Irminger Sea. **(E)** Greenland GISP-2 $\delta^{18}O$ record (*11*). Timing of large meltwater Heinrich events (H2 to H6) from (*3, 4, 14*). The North Atlantic records (C and D) track the south-north oscillations of the polar front for all D-0 events. Each record has its own dynamic, but strong links are demonstrated by their detailed similarity.

To determine the correct mechanism, it is important to show whether the low-latitude changes lead or lag those in the high latitudes. This is why high resolution and accurate dating are so important. The Cariaco Basin is very interesting in this regard. Isolated from the open ocean by a shallow sill, it reflects only the characteristics of the upper ocean. Its bottom waters are often insufficiently ventilated and become anoxic. The basin does not support an active benthic fauna, and sediments show annually resolved layering during the anoxic periods (particularly for the past 15,000 years). Furthermore, the basin is directly influenced by the northeast trade winds and the oscillations of the ITCZ and is thus well situated for studying their variability during D-O events.

Hughen *et al.* (*1*) and Peterson *et al.* (*2*) report important new results from Cariaco Basin sedimentary records. Hughen *et al.* (*1*) present an impressive high-resolution accelerator mass spectrometry (AMS) ^{14}C record that provides a high-precision calibration for converting radiocarbon dates to calendar years for the period from 15 to 10 ka. They also demonstrate, in unprecedented detail, to what extent CO_2 transfer between ocean and atmosphere changes during times of rapid climatic change and determine the contribution of these changes to ^{14}C variability.

Using their new ^{14}C calibration, Hughen *et al.* build a very precise (calendar year) time scale for the Cariaco Basin records for the period of the Younger Dryas. This gives an excellent high-resolution record on the same time scale (within a few decades) as the Greenland Ice Sheet Project (GISP) record. Interpretation is hampered, however, by the use of a relatively qualitative proxy temperature record, "gray scale." Modern analogy would indicate that the lighter sediment during the Younger Dryas corresponds to high upwelling activity and high trade wind intensity over the Southern Caribbean Sea (*9*). This would fit with Rühlemann's reconstruction of warmer sea surface temperature in the western tropical Atlantic for that period (*7*), but only if stronger trade winds are linked to a more pronounced warm pool in the area.

Peterson *et al.* (*2*) explore a longer part of the Cariaco record spanning most of the past 90 ka. Here, no direct continuous interannual layer counting is possible. To establish a time scale for their record, the authors assume that the climatic relation between the Cariaco and Greenland records remains the same for the whole glacial period as during the Younger Dryas. The cold events in the GISP-2 record are thus assumed to be in phase with the light parts of the Cariaco record. The corresponding correlation is impressive, although we should remember the absence of independent absolute dating. A high-resolution determination of the iron and titanium content of the sediments demonstrates that the sediment flux from the nearby continent alternates between high and low throughout the record. High fluxes correspond to periods of increased rainfall and are in phase with the warm periods in GISP-2.

Peterson *et al.* suggest that the increase in rainfall corresponds, as for the modern summer, to the passage of the thermic equator (the ICTZ) at the latitude of the Cariaco Basin. This is also the latitude of the Panama Isthmus, where maximum transfer of water vapor to the Pacific Ocean could occur, thus increasing the mean salinity of the Atlantic warm pool. Warm D-O events would then be reinforced by the increased salt content in the source water for the North Atlantic thermohaline convection.

This is an interesting hypothesis, but this feedback effect would probably be negligible over the short warming phase (see the figure). The temporal relation between low-latitude forcing and the evolution of the northern ice sheets, wind field, and thermohaline circulation is therefore still not known at sufficient resolution (a few decades) to establish the D-O mechanism. We need to use better paleoclimatic proxies, especially to quantify sea surface temperature, and more high sedimentation rate cores, in particular in the Gulf of Mexico. Hydrological changes in the Gulf Stream source waters must also be characterized better if we want to understand the role of the thermohaline circulation in rapid climate change.

References and Notes

1. K. A. Hughen, J. R. Southon, S. J. Lehman, J. T. Overpeck, *Science* **290**, 1951 (2000).
2. L. C. Peterson, G. H. Haug, K. A. Hughen, U. Röhl, *Science* **290**, 1947 (2000).
3. G. Bond *et al.*, *Nature* **365**, 143 (1993).
4. E. Cortijo *et al.*, *Earth Planet. Sci. Lett.* **146**, 29 (1997).
5. L. Vidal *et al.*, *Earth Planet. Sci. Lett.* **146**, 13 (1997).
6. T. L. Rassmussen, T. C. E. Van Weering, L. Labeyrie, *Quat. Sci. Rev.* **16**, 71 (1997).
7. C. Rühlemann *et al.*, *Nature* **402**, 511 (1999).
8. See http://www.images.cnrs-gif.fr
9. K. A. Hughen, J. T. Overpeck, L. C. Peterson, S. Trumbore, *Nature* **380**, 51 (1996).
10. P. M. Grootes, M. Stuiver, *J. Geophys. Res.* **102**, 26455 (1997).
11. P. M. Grootes *et al.*, *Nature* **366**, 552 (1993).
12. I. L. Hendy, J. P. Kennett, *Geology* **27**, 291 (1999).
13. N. J. Shackleton, M. A. Hall, E. Vincent, *Paleoceanography*, in press.
14. S. van Krevelt *et al.*, *Paleoceanography* **15**, 425 (2000).
15. Institut Français de Recherche et Technologie Polaire is acknowledged for its large support of the IMAGES Marion Dufresne (MD) cruises.

PERSPECTIVES: OPTICS

The Internet of Tomorrow

Steve Joiner

The digital economy is generating an insatiable appetite for bandwidth. Internet traffic now hits daily peaks of 0.47 terabits per second and is expected to increase by more than an order of magnitude to 5.64 terabits per second by the end of 2001 (*1*). The data moved around the globe are getting richer and more dynamic with each passing day, and an increasingly impatient public expects faster and faster responses. This endless demand is creating stress points that threaten to make the Web's infrastructure collapse under the weight of its own success.

The problem does not lie with data transfer from city to city or even across continents or oceans. Because of advances in dense wave-division multiplexing technology, which enables the creation of multiple communication paths on one fiber through the use of multiple wavelengths of light in the fiber, fiber communication capacity has doubled every nine months. The increased capacity of the fiber enables much more efficient use of installed fiber, thus lowering operating costs for long-haul optical communication.

The real bottleneck today is the access network that extends from the desktop to the service provider's Internet point of presence (see the figure). This "short reach" or "last mile" still uses the installed base of traditional copper connections or the copper used in cable TV systems. The new high-speed Internet connections based on cable modems or digital subscriber line (DSL) both rely on fiber connections terminating relatively close to the end user. The optical connections used in these cases are becoming more economical as volumes increase. Thus, optics is beginning to solve today's "last-mile" bandwidth bottleneck.

In the near future, the bottlenecks choking the Internet will be even closer to home: the very short-reach interfaces that connect buildings, floors, racks, storage subsystems, internal computer components, and even the onboard elements of integrated circuits. If the Internet is to continue its explosive growth, optical elements must be scaled down and applied at these levels. One of the most promising technologies is a relative newcomer, the vertical cavity surface emitting laser (VCSEL).

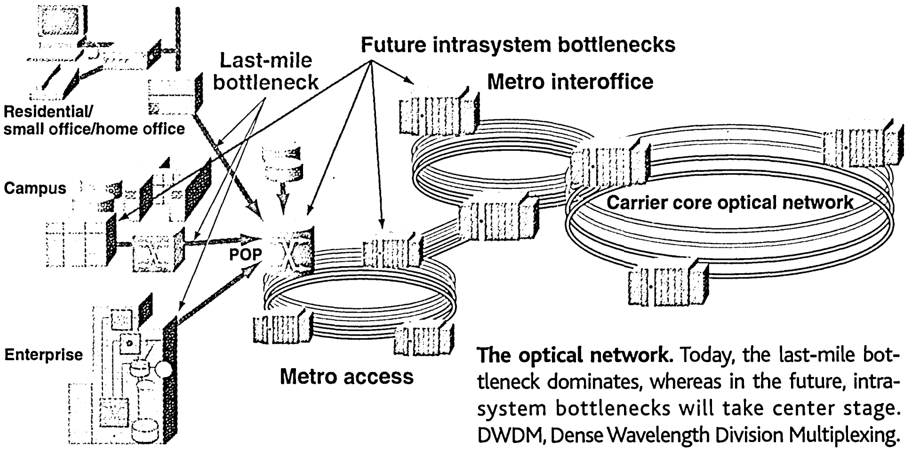

The optical network. Today, the last-mile bottleneck dominates, whereas in the future, intrasystem bottlenecks will take center stage. DWDM, Dense Wavelength Division Multiplexing.

Traditional lasers are edge-emitting, whereas VCSELs emit light from their top surface in a cylindrical beam. This has the advantage that the emitted light requires no corrections for asymmetry or astigmatism and can be shaped into a ring for various applications. VCSELs are also very efficient, requiring just a fraction of the power used by edge-emitting lasers, thus simplifying the electronic circuitry that drives them and reducing radio frequency interference (RFI) emissions. And VSCELs are smaller than conventional lasers: The entire VCSEL can be shrunk until it is only slightly larger than the beam size.

Surface emission also allows for easier mounting and packaging. VCSELs can be attached flat onto the package substrate by the same type of equipment used to assemble integrated circuits and can be tested directly on the wafers. Separating the lasers from the wafers and packaging them into arrays becomes trivial, the yield per wafer is a much higher, and the packing density increases by an order of magnitude—a critical capability for constructing high-speed optical interconnects for computer systems and networks. All these factors reduce development and manufacturing costs and move the benefits of optics closer to the consumers.

As the data traffic from the desktop is routed through the network and aggregated with other traffic in the backbone of the Internet, the traffic inside the routing switches will increase to the point that electrical connections will not work even over distances covering a single piece of networking equipment. Manufacturers are turning

---

The author is with Agilent Laboratories, 3500 Deer Creek Road, MS 26M, Palo Alto, CA 94304, USA. E-mail: steve_joiner@agilent.com